Theor Chem Account (2007) 118:681–691
DOI 10.1007/s00214-007-0363-x

REGULAR ARTICLE

Multiresolution potential energy surfaces for vibrational state calculations

Kiyoshi Yagi · So Hirata · Kimihiko Hirao

Received: 29 November 2006 / Accepted: 22 January 2007 / Published online: 20 July 2007

Abstract A compact and robust many-mode expansion of potential energy surfaces (PES) is presented for anharmonic vibrations of polyatomic molecules, where the individual many-mode terms are approximated with various different resolutions, i.e., electronic structure methods, basis sets, and functional forms. As functional forms, the following three representations have been explored: numerical values on a grid, cubic spline interpolation, and a Taylor expansion. A useful index is proposed which rapidly identifies important many-mode terms that warrant a high resolution. Applications to water and formaldehyde demonstrate that the present scheme can increase the efficiency of the PES computation by a factor of up to 11 with the errors in anharmonic vibrational frequencies being no worse than $\sim 10\,\mathrm{cm}^{-1}$.

1 Introduction

Recent advances in molecular theory have made it feasible to simulate anharmonic rovibrational spectra of polyatomic molecules from the first principles [1]. The vibrational self-consistent field (VSCF) method [2,3] provides a means to find the variationally "best" one-mode functions in which the total vibrational wavefunction is constructed as their product. The dimensionality of the Schrödinger equation is greatly reduced by dividing the fully coupled equation to many one-mode equations with associated effective one-dimensional potential energy curves. However, the effective potential derived from a full dimensional PES still suffers from the high dimensionality of the system. Carter et al. [8] have introduced a hierarchical expansion of the PES in terms of the couplings among the normal coordinates (see Eq. (1)). This expansion of the PES is rapidly convergent typically at $n = 2 - 4$, reducing the computational cost of its evaluation from M^f to M^n, where M is the number of grid points along a normal coordinate and f is the number of internal degrees of freedom. The truncated PES can be obtained either by on-the-fly ab initio electronic structure calculations at every grid point [9–12] or by ab initio derived potential energy functions (PEFs) [13–34]. The VSCF method and its extensions [4–7] combined with the electronic structure theory have enabled the vibrational structure calculations of polyatomic molecules.

In spite of its singular importance, Carter and co-workers' n-mode representation (nMR) method can be further enhanced. The nMR method, as it is implemented, treats all the vibrational modes and couplings in an equal manner and uses the same level of electronic structure methods and functional forms for all. As a result, the computational efforts are devoted mostly for evaluating numerous higher order coupling terms. This is a wasteful procedure since these terms are almost always less important compared to the leading, lower order coupling terms. Furthermore, in complex systems, we often place emphasis on a specific mode of interest rather than on the whole feature of the spectrum, again suggesting the use of different treatments for different orders of coupling. It is hence desirable to have an extended nMR-PES that incorporates multiple resolutions (collectively referring to the level of electronic structure theory, basis set size, functional forms

K. Yagi · K. Hirao (✉)
Department of Applied Chemistry, School of Engineering,
The University of Tokyo, Tokyo 113-8656, Japan
e-mail: hirao@qcl.t.u-tokyo.ac.jp

K. Yagi · K. Hirao
CREST, Japan Science and Technology Agency,
Saitama 332-0012, Japan

S. Hirata
Quantum Theory Project, Department of Chemistry,
University of Florida, Gainesville, FL 32611-8435, USA

of the surface, etc.), where important terms are determined at higher resolutions and less important ones at progressively lower resolutions. In other words, in addition to truncating the series of expansion of PES according to dimensionality, we should adjust or even optimize the resolution for each expansion term according to its importance.

The idea of using multiresolution in approximating the PES has been explored by several researchers. Bürger et al. [18,19], Boese and Martin [20], and Begue et al. [21] employed dual level approaches in deriving the quartic force field: an accurate and expensive electronic structure method for harmonic force constants and an approximate method for anharmonic force constants. Carter and co-workers have extended the original *n*MR-PES by introducing the "intrinsic" *n*-mode coupling terms each of which can be determined with different accuracy (or grid) based on least square fittings [24] or Hermite interpolations [25]. They showed that the numbers of data points along each normal mode for three- and four-mode coupling terms can be only one quarter of those of one- and two-mode coupling terms without deteriorating the quality of the results significantly. In their paper, the use of multiple electronic structure levels was also suggested, but not implemented. The most thorough investigation in this direction thus far has been conducted by Rauhut [26]. In this work, two different electronic structure levels were employed to compute different intrinsic *n*-mode coupling terms. Later this dual-level approach was extended to multi levels by Rauhut's group [27,28]. In addition, he explored highly effective strategies to minimize the computational cost of generating PES by introducing an automatic and iterative fitting procedure of the higher order surfaces with minimal number of data points and surface area. Together with a convenient pre-screening criterion, Rauhut was able to achieve the remarkable speedup by a factor of 18,000 in generating PES of 1,2,5-oxadiazole (a 7-atom system) relative to a conventional method.

Following these preceding works, we examine the usage of further flexible resolutions to represent the intrinsic *n*-mode coupling terms. The strongly anharmonic terms are determined with high resolutions, i.e., by accurate functions and electronic structure methods, while the others are evaluated in a more approximate way, for example, by the quartic force field (QFF) derived from a lower level of theory. It is known that QFF reliably represents moderate anharmonicities and is rapidly computable especially when analytic Hessians are available [13–22]. For this purpose, we first show that the intrinsic mode coupling terms are obtained independently from a reduced dimensional PEF determined at an arbitrary resolution. The explicit forms of the piecewise PEF are then explored, i.e., grid representations, interpolation functions, and Taylor series expansions. These functions can be determined by various electronic structure theories ranging from coupled-cluster to density functional theory. The mixed usage of the above functions in representing the *n*MR-PES is new in the multiresolution context and is shown to be highly effective.

It is essential to distinguish the important mode coupling terms from the others in advance of the full calculation of the PES in actual implementations of the above scheme. For this, we propose a rapidly computable index that roughly estimates the strength of mode coupling terms. With the aid of this index, we can introduce multiresolution within one *n*-mode coupling term: for example, a higher resolution for important three-mode terms and a lower resolution for less important three-mode terms. Furthermore, we examine the use of normal coordinates determined by the lower level of electronic structure theory to represent the anharmonic potential, which enables to bypass the calculations of equilibrium geometry and Hessian matrix at a higher level of theory. This scheme has been successfully employed by Rheinecker and Bowman to generate the potential energy and dipole moment surfaces in simulating the infrared spectrum of Cl^-H_2O cluster [33,34]. It is also shown in this work that the vibrational frequencies obtained from this scheme incur only small deviations from those of the conventional method.

2 Multiresolution PES

2.1 Construction of the *n*MR-PES from piecewise PEFs

In the VSCF method, the potential energy surface (PES) of f mode systems is expanded in terms of mode couplings as [8],

$$\begin{aligned} V(\mathbf{Q}) = &\sum_{i_1} V_{i_1}(Q_{i_1}) + \sum_{i_1<i_2} V_{\mathbf{i}_2}(Q_{i_1}, Q_{i_2}) \\ &+ \cdots + \sum_{i_1<\cdots<i_m} V_{\mathbf{i}_m}(Q_{i_1}, \ldots, Q_{i_m}) \\ &+ \cdots + V_{\mathbf{i}_f}(Q_1, \ldots, Q_f), \end{aligned} \tag{1}$$

where Q_i is the ith normal coordinate, $\mathbf{i}_m$ denotes a compound index of $(i_1 i_2 \cdots i_m)$, and $V_{\mathbf{i}_m}$ represents an m-mode coupling term,

$$\begin{aligned} V_{\mathbf{i}_m}(Q_{i_1}, \ldots, Q_{i_m}) = &V(0, \ldots, 0, Q_{i_1}, 0, \ldots, 0, \\ &Q_{i_m}, 0, \ldots, 0) \\ &- \sum_{l=1}^{m-1} \sum_{\mathbf{i}_l \in \mathbf{i}_m} V_{\mathbf{i}_l}(Q_{i_1}, \ldots, Q_{i_l}). \end{aligned} \tag{2}$$

Note that the energy at the origin is set to zero, $V(\mathbf{0}) = 0$. The mode coupling terms satisfy the following relation (a proof given in the appendix),

$$V_{\mathbf{i}_m}(Q_{i_1}, \ldots, Q_{i_m}) = 0, \quad \text{if any } Q_{i_k} = 0. \tag{3}$$

This relation ensures the mode-coupling expansion in Eq. (1) to exactly reproduce the full dimensional PES at the fth order. The PES truncated at the nth order is referred to as an n-mode representation of the PES (nMR-PES),

$$V(\mathbf{Q}) \simeq V^{n\mathrm{MR}}(\mathbf{Q}) = \sum_{i_1} V_{i_1}(Q_{i_1}) + \sum_{i_1<i_2} V_{\mathbf{i}_2}(Q_{i_1}, Q_{i_2}) + \sum_{i_1<i_2<i_3} V_{\mathbf{i}_3}(Q_{i_1}, Q_{i_2}, Q_{i_3}) + \cdots + \sum_{i_1<\cdots<i_n} V_{\mathbf{i}_n}(Q_{i_1}, \ldots, Q_{i_n}). \quad (4)$$

It is desirable to express this nMR-PES equation in such a way that mode coupling terms can be determined at different approximations of the electronic structure theory and different functional forms; for example, low-order terms with large contributions by more accurate, expensive methods, and high-order terms by more approximate, inexpensive methods. The conventional formalism, however, does not immediately allow such a treatment because each mode coupling term defined recursively by Eq. (2) does no longer satisfy the condition (3) when more than one resolutions are used.

"Intrinsic" n-mode coupling term enables to circumvent this problem [24–26]. Consider a set of piecewise reduced dimensional PEFs $\{F_{\mathbf{i}_m}(Q_{i_1}, \ldots, Q_{i_m})\}$, each of which approximately represents a subspace of the configuration space associated with one resolution (e.g., a certain electronic structure method and functional form). The intrinsic m-mode coupling term is obtained from $F_{\mathbf{i}_m}$ as

$$G_{\mathbf{i}_m}(Q_{i_1}, \ldots, Q_{i_m}) = F_{\mathbf{i}_m}(Q_{i_1}, \ldots, Q_{i_m}) - \sum_{l=1}^{m-1} \sum_{\mathbf{j}_l \in \mathbf{i}_m} g^{\mathbf{j}_l}_{\mathbf{i}_m}(Q_{j_1}, \ldots, Q_{j_l}), \quad (5)$$

where $g^{\mathbf{j}_l}_{\mathbf{i}_m}$ represents an l-mode coupling term of $F_{\mathbf{i}_m}$,

$$g^{\mathbf{j}_l}_{\mathbf{i}_m}(Q_{j_1}, \ldots, Q_{j_l}) = F_{\mathbf{i}_m}(0, \ldots, 0, Q_{j_1}, 0, \ldots, 0, Q_{j_l}, \ldots, 0) - \sum_{l'=1}^{l-1} \sum_{\mathbf{j}_{l'} \in \mathbf{j}_l} g^{\mathbf{j}_{l'}}_{\mathbf{i}_m}(Q_{j_1}, \ldots, Q_{j_{l'}}), \quad (6)$$

determined at one resolution. Note that $G_{\mathbf{i}_m} = g^{\mathbf{i}_m}_{\mathbf{i}_m}$. For example, the intrinsic one-, two-, and three-mode coupling terms are written as,

$$G_i(Q_i) = F_i(Q_i), \quad (7)$$

$$G_{ij}(Q_i, Q_j) = F_{ij}(Q_i, Q_j) - F_{ij}(Q_i, 0) - F_{ij}(0, Q_j), \quad (8)$$

$$G_{ijk}(Q_i, Q_j, Q_k) = F_{ijk}(Q_i, Q_j, Q_k) - F_{ijk}(Q_i, Q_j, 0) - F_{ijk}(Q_i, 0, Q_k) - F_{ijk}(0, Q_j, Q_k) + F_{ijk}(Q_i, 0, 0) + F_{ijk}(0, Q_j, 0) + F_{ijk}(0, 0, Q_k). \quad (9)$$

It is of particular importance that each term is associated with a single PEF and assigned the resolution on which the PEF is based.

It can be easily verified that the intrinsic mode coupling term satisfies the condition (3),

$$G_{\mathbf{i}_m}(Q_{i_1}, \ldots, Q_{i_m}) = 0, \quad \text{if any } Q_{i_k} = 0. \quad (10)$$

Thus, these terms, obtained from the set of PEFs, $\{F_{\mathbf{i}_m}\}$, can be summed to give an extended nMR-PES as,

$$V^{n\mathrm{MR}}(\mathbf{Q}) = \sum_{i_1} G_{i_1}(Q_{i_1}) + \sum_{i_1<i_2} G_{\mathbf{i}_2}(Q_{i_1}, Q_{i_2}) + \cdots + \sum_{i_1<\cdots<i_n} G_{\mathbf{i}_n}(Q_{i_1}, \ldots, Q_{i_n}). \quad (11)$$

Note that Eq. (10) ensures the correct behavior of the nMR expansion at the limit. Each term in Eq. (11) can now be determined with different resolutions enabling the multiresolution nMR-PES. This scheme reduces to the original nMR-PES when one resolution is used for all the terms.

As mentioned above, the use of multiple resolutions is not permitted in the original nMR-PES due to the dependence of the high-order terms on the lower order terms (Eq. (2)). We assume that the previous works on multiresolution nMR-PES [24–26] are based on Eq. (5) instead of Eq. (2), since otherwise the expansion would break down both conceptually and numerically. To our best knowledge, however, the difference between the two schemes has not been clearly stated before the present work. Here, the extended nMR-PES is presented through Eq. (5), which gives an actual procedure to compute the mode coupling terms at different resolutions, together with an emphasis on the condition (10) to achieve the correct nMR expansion. Following the convention, we term $G_{\mathbf{i}_m}$ the "intrinsic" mode coupling term.

2.2 Practical forms of the piecewise PEFs

In practical implementations, the explicit functional forms of the piecewise PEFs need to be specified. There are a number of candidates that may be used for the present purpose, and the search for optimal forms as well as their combinations is an important issue. Here, we explore several forms that are found useful in the subsequent applications.

2.2.1 Direct PEF on the grid

In VSCF solvers, the potential energy values are required at numerical grid points, the distribution of which is determined by, for example, the discrete variable representation (DVR) method [35]. These energy values can be obtained on-the-fly from electronic structure calculations. These data points may be regarded as a PEF in a grid representation, which is denoted as direct PEF in the following. Direct PEF

is exact in the sense that it does not rely on any assumed functional form. If all the mode coupling terms in nMR-PES are derived from direct PEF of the same ab initio quality, the VSCF based on this PES reduces to the direct VSCF method [9–12]. Its application, however, is severely limited due to the exponential increase in the number of grid points with respect to the dimension of the PEF (m) as M^m, where M is the number of grid points along each normal coordinate. It is prohibitive to calculate direct PEFs for the higher order coupling terms ($m \geq 4$), even with inexpensive electronic structure methods. Direct PEF can most suitably represent a few, very important, low-order coupling terms. In the present study, 1MR terms are always derived from direct PEFs.

2.2.2 Interpolation functions

The regions of the PES far from the equilibrium geometry usually have smaller influence on the low-lying vibrational energies and wavefunctions. This fact suggests the use of a more approximate treatment for less important regions of the PES. Previously, several authors have proposed to use interpolation [25,26] or fitting [24] functions to represent the piecewise PEFs. The scheme that incorporates the derivatives of the PES [23,29] may also be a good candidate.

In this study, we have employed a standard cubic spline interpolation technique to represent the piecewise PEFs. The m-dimensional PEF is generated from recursive spline interpolations of one-dimensional cuts with x grid points along each normal coordinate (denoted Sx). The construction of Sx needs potential energy values at x^m grid points, so that a considerable saving of the computational cost can be achieved by adopting $x < M$, though the unfavorable scaling with respect to the dimension m is not removed. The interpolation points must be carefully selected, for the resulting vibrational frequencies are very sensitive to their positions. Preliminary calculations have yielded the best performance when these points are placed according to the Gauss–Hermite quadrature (perhaps, placing at the DVR grid points is generally effective). In this way, the use of spline functions obtained with M interpolation points is mathematically equivalent to the use of energy values at the original numerical grid, i.e., direct PEF. The question is, therefore, how accurate are the PEFs interpolated with the smaller grid (x^m) relative to the ones defined for the original grid (M^m).

2.2.3 Taylor expansion PEF

The mode coupling terms may be alternatively written in a Taylor series expansion as,

$$G_{\mathbf{i}_m}(Q_{i_1}\cdots Q_{i_m}) = \sum_{\mathbf{k}_m}^{\infty} \frac{c_{\mathbf{k}_m} Q_{i_1}^{k_1}\cdots Q_{i_m}^{k_m}}{k_1!\cdots k_m!}, \tag{12}$$

where the coefficients, $c_{\mathbf{k}_m}$, are the derivatives of the PES at the equilibrium geometry with respect to normal coordinates. If the expansion is truncated at the fourth-order, i.e., $\sum_j^m k_j \leq 4$, then Eq. (12) reduces to the quartic force field (QFF) [13–22]. In this case, the mode coupling terms are written as

$$G_i^{\mathrm{QFF}} = \frac{1}{2}c_{ii}Q_i^2 + \frac{1}{6}c_{iii}Q_i^3 + \frac{1}{24}c_{iiii}Q_i^4, \tag{13}$$

$$G_{ij}^{\mathrm{QFF}} = \frac{1}{2}(c_{iij}Q_i^2Q_j + c_{ijj}Q_iQ_j^2) + \frac{1}{6}(c_{iiij}Q_i^3Q_j + c_{ijjj}Q_iQ_j^3) + \frac{1}{4}c_{iijj}Q_i^2Q_j^2, \tag{14}$$

$$G_{ijk}^{\mathrm{QFF}} = c_{ijk}Q_iQ_jQ_k + \frac{1}{2}(c_{iijk}Q_i^2Q_jQ_k + c_{ijjk}Q_iQ_j^2Q_k + c_{ijkk}Q_iQ_jQ_k^2), \tag{15}$$

$$G_{ijkl}^{\mathrm{QFF}} = c_{ijkl}Q_iQ_jQ_kQ_l. \tag{16}$$

The third- and fourth-order derivatives, c_{ijk} and c_{ijkl}, can be computed by numerical differentiations of the energy [16], or the Hessian matrix [11]. QFF is valid by definition only near the origin (within the convergence radius), and may not be suitable to represent strongly anharmonic terms or to be used in calculations of highly excited states. Nevertheless, the advantage of QFF lies in its capability to reproduce numerous, moderate anharmonicity with a much less computational cost compared to direct PEF and interpolation PEF.

It is also important to note that the Taylor expansion PEF can be integrated with much less computational cost, where the multidimensional integral can be evaluated by a product of one-dimensional integrals over the one-mode functions. A fast integration algorithm will make it easier to incorporate the higher order terms in the vibrational state calculations.

2.3 Detection of the strength of mode coupling terms

The number of n-mode coupling terms increases very rapidly with the vibrational degrees of freedom (f) as $\sim f^n$. Therefore, it is important to devise a simple index which inexpensively permits identifying the important terms that should be evaluated at a high resolution from the others that can be obtained at a lower resolution. The strength of mode coupling terms is determined by the two factors: the strength of anharmonicity and the resonance condition.

Let us first consider the former. Define two grid points along each normal coordinate denoted $Q_i^{(+)}$ and $Q_i^{(-)}$ for the ith mode as,

$$Q_i^{(\pm)} = \pm\sqrt{\frac{2\hbar}{\omega_i}}, \tag{17}$$

where ω_i denotes the harmonic frequency of the ith mode. Note that the harmonic potential gives an energy of $\hbar\omega_i$

at these positions, i.e., $Q_i^{(+)}$ takes a small value for high frequency modes, and vice versa. Together with the origin, the energy values at the 3^n grid points are computed by the electronic structure calculations to evaluate the n-mode coupling terms on the grid. The strength of the anharmonic potential may be expressed as an average of these values over the grid. For two-mode coupling terms, for example, the index is given as

$$\sigma_{ij}^{(\alpha,\beta)} = E(Q_i^{(\alpha)}, Q_j^{(\beta)}) - E(Q_i^{(\alpha)}, 0) - E(0, Q_j^{(\beta)}), \quad (18)$$

$$\sigma_{ij} = \frac{1}{2^2}\left|\sum_{\alpha,\beta}\sigma_{ij}^{(\alpha,\beta)}\right|, \quad (19)$$

where α and β denote the signs. The indices for higher order terms can be defined analogously as,

$$\sigma_{\mathbf{i}_n} = \frac{1}{2^n}\left|\sum_{\alpha,\beta,\ldots,\gamma}\sigma_{\mathbf{i}_n}^{(\alpha,\beta,\ldots,\gamma)}\right|. \quad (20)$$

The resonance condition for the two- and three-mode coupling terms is met when,

$$\hbar\delta_{ij} = \frac{1}{2!}\frac{1}{|2\omega_i - \omega_j|} + \frac{1}{3!}\frac{1}{|3\omega_i - \omega_j|} + \frac{1}{3!}\frac{1}{|\omega_i - \omega_j|} + \frac{1}{4!}\frac{1}{|4\omega_i - \omega_j|} + \frac{1}{4!}\frac{1}{|2\omega_i - \omega_j|}, \quad (21)$$

$$\begin{aligned}\hbar\delta_{ijk} = {} & \frac{1}{|\omega_i + \omega_j - \omega_k|} \\ & + \frac{1}{2!}\left[\frac{1}{|\omega_i + 2\omega_j - \omega_k|} + \frac{1}{|2\omega_i + \omega_j - \omega_k|}\right] \\ & + \frac{1}{3!}\left[\frac{1}{|3\omega_i + \omega_j - \omega_k|} + \frac{1}{|\omega_i + 3\omega_j - \omega_k|}\right] \\ & + \frac{1}{3!}\left[\frac{1}{|\omega_i + \omega_j - \omega_k|} + \frac{1}{|\omega_i + \omega_j - \omega_k|}\right] \\ & + \frac{1}{2!2!}\frac{1}{|2\omega_i + 2\omega_j - \omega_k|}. \end{aligned} \quad (22)$$

In our implementations, a small number ($\sim$10 cm^{-1}) is added to the denominator to avoid a division by zero. Finally, the proposed index is expressed as

$$\xi_{\mathbf{i}_n} = \sigma_{\mathbf{i}_n} \times \delta_{\mathbf{i}_n}. \quad (23)$$

Note that the index is a dimensionless number. Although additional costs are incurred by the calculation of the energy on the grid, these indices are relatively insensitive to the level of electronic structure theory employed, and hence can be estimated at a low-level electronic structure theory.

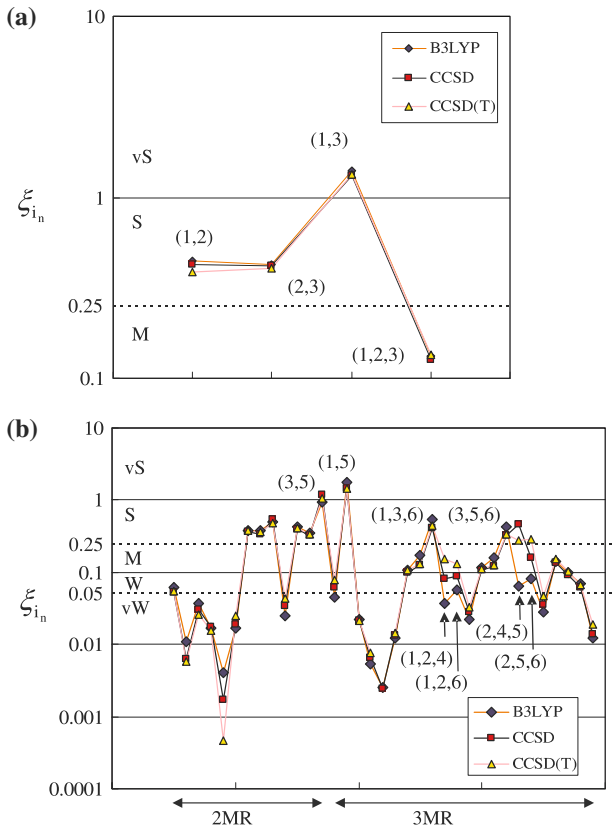

Fig. 1 The proposed indices detecting the importance of mode coupling terms obtained by the B3LYP/cc-pVDZ, CCSD/cc-pVDZ, and CCSD(T)/cc-pVTZ level of theory, for **a** H_2O and **b** H_2CO

3 Applications

3.1 Strength of mode coupling terms

We first examine the strength of mode coupling terms in H_2O and H_2CO using the indices proposed in the previous section. The equilibrium geometry and the harmonic frequencies of H_2O and H_2CO were first computed by the B3LYP [36,37], CCSD [38,39], and CCSD(T) levels of theory. The B3LYP and CCSD calculations were performed with the cc-pVDZ [40] basis sets, and the CCSD(T) calculation with the cc-pVTZ basis sets. The core orbital of oxygen and carbon was kept frozen in the coupled-cluster calculations. In the present work, all coupled-cluster calculations were performed using the ACES II program package [41], and the B3LYP calculations by using the GAUSSIAN 03 program package [42]. The resulting normal coordinates and harmonic frequencies were employed to calculate the indices for the two- and three-mode coupling terms; 27 and 232 points of ab initio energy were required to evaluate the strength of the anharmonic potential of H_2O and H_2CO, respectively. Figure 1 presents the indices for these molecules obtained by the B3LYP/cc-pVDZ, CCSD/cc-pVDZ, and CCSD(T)/cc-pVTZ level of theory. It

Table 1 The two- and three-mode coupling terms of H_2O and H_2CO classified into five categories based on the proposed index (ξ) obtained by the B3LYP/cc-pVDZ level of theory

	H_2O		H_2CO			
	Term	ξ	Term	ξ	Term	ξ
vS[a] (>1)	(1,3)	1.391	(1,5)	1.769		
S[b] (0.25–1)	(1,2)	0.442	(3,5)	0.949	(4,5)	0.425
	(2,3)	0.427	(1,3,6)	0.551	(1,4)	0.382
			(1,3)	0.505	(1,6)	0.374
			(3,5,6)	0.434	(5,6)	0.356
M[c] (0.1–0.25)	(1,2,3)	0.133	(1,3,4)	0.169	(4,5,6)	0.115
			(3,4,5)	0.158	(1,4,6)	0.109
			(1,4,5)	0.143	(1,5,6)	0.100
W[d] (0.05–0.1)			(2,5,6)	0.082	(4,6)	0.062
			(1,3,5)	0.071	(1,2,6)	0.057
			(2,4,5)	0.064		
vW[e] (<0.05)			(2,5)	0.046	(2,3)	0.017
			(1,2,4)	0.037	(1,2,5)	0.012
			(3,6)	0.037	(2,3,6)	0.012
			(2,3,5)	0.028	(3,4)	0.011
			(1,2)	0.025	(2,4,6)	0.005
			(1,2,3)	0.023	(2,6)	0.004
			(3,4,6)	0.022	(2,3,4)	0.003
			(2,4)	0.017		

[a] Very Strong
[b] Strong
[c] Medium
[d] Weak
[e] Very Weak

is observed that appreciable deviations are found only for four three-mode coupling terms of H_2CO, (Q_1, Q_2, Q_4), (Q_1, Q_2, Q_6), (Q_2, Q_4, Q_5), and (Q_2, Q_5, Q_6), which are caused due to the accidental near degeneracy of these combinations; for example, $|\omega_5 - \omega_4 - \omega_2|$ is obtained as 101, 7, and 25 cm^{-1} by B3LYP, CCSD, and CCSD(T), respectively. The indices are almost insensitive to the level of theory employed, and hence can be reliably evaluated by a low-level of electronic structure method (e.g., B3LYP/cc-pVDZ).

The mode coupling terms of H_2O and H_2CO are classified into five categories according to the indices obtained by the B3LYP/cc-pVDZ method as presented in Table 1: (1) Very Strong ($\xi > 1$), (2) Strong ($0.25 < \xi < 1$), (3) Medium ($0.1 < \xi < 0.25$), (4) Weak ($0.05 < \xi < 0.1$), and (5) Very Weak ($\xi < 0.05$). "Very strong" mode couplings are, as expected, found for the one between the symmetric and anti-symmetric stretching modes of the OH and CH bonds characterized by $\xi_{13} = 1.391$ and $\xi_{15} = 1.769$, respectively. Two three-mode terms of H_2CO, (Q_1, Q_3, Q_6) and (Q_3, Q_5, Q_6), are found as "strong" terms. The latter is a very important term which directly contributes to Fermi resonance between ν_5 and $\nu_3 + \nu_6$ (see below). It is also interesting to note that the index for the three-mode term, ξ_{ijk}, trends to be smaller than ξ_{ij}, ξ_{ik}, and ξ_{jk}. This observation is consistent with Rauhut's pre-screening condition [26] in which the three-mode term, (i, j, k), is neglected if the associated pairs, (i, j), (j, k), and (k, l), are smaller than a screening threshold. For larger molecules, it may be useful to combine this condition with the present scheme.

3.2 Vibrational state calculations

3.2.1 Direct VCI calculations

The anharmonic vibrational wavefunctions and frequencies were first calculated by the direct VSCF and vibrational configuration interaction (VCI) method [11] using the SINDO program [43]. The number of points in a Gauss–Hermite quadrature grid was set to 11 for each coordinate, and ab initio energies for the 3MR-PES were calculated at 1,331 and 21,566 numerical grid points for H_2O and H_2CO, respectively, at the CCSD(T)/cc-pVTZ level of theory. The energy on the grid was scanned by the SINDO program, which made use of the molecular symmetry (C_{2v}) to avoid unnecessary electronic structure calculations at symmetrically nonunique points. It also had a fault recovery measure, which automatically interpolated or extrapolated the energies when energy calculations failed at highly strained geometries. In H_2O, 500 low-lying VSCF configurations were selected for VCI calculations. VCI calculations for H_2CO were carried out by selecting the VSCF configurations such that each quantum number was excited up to 6, and the sum of all quantum number was less than 6 (924 configurations in total). The lowest lying 14 and 80 vibrational states have been computed for H_2O and H_2CO, respectively, by direct VCI method based on the 2MR- and 3MR-PES. The results of direct VCI/3MR calculation serve as reference values for the following calculations with approximate PESs.

3.2.2 Multiresolution PES

Multiresolution PESs (MultiR-PES) for H_2O and H_2CO have been constructed by combining mode coupling terms derived from various resolutions (functional form and electronic structure method). In view of the proposed index, one resolution was assigned to each category of the mode coupling term presented in Table 1. More specifically, the one-mode terms and the "very strong" mode coupling terms were represented by direct PEF (i.e., S11) at the CCSD(T)/cc-pVTZ level of theory (denoted direct/CCSD(T)/cc-pVTZ), the "strong" terms by S9/CCSD(T)/cc-pVTZ, the "medium" terms by S7/CCSD/cc-pVDZ, the "weak" terms by S5/B3LYP/cc-pVDZ, and the "very weak" terms by QFF/B3LYP/cc-pVDZ. QFF was constructed by numerical differentiations of the

Table 2 Vibrational energy levels of H_2O obtained from the VCI method based on two types of multiresolution PES (MultiR-PES), together with direct VCI/2MR and 3MR results, and the experimental values

	MultiR-PES1[a]	MultiR-PES2[b]	Direct2MR	Direct3MR	Exp.[c]
ν_2	1604.5 (0.1)	1604.3 (0.2)	1601.6 (2.9)	1604.4	1594.7
$2\nu_2$	3172.8 (0.0)	3172.2 (0.6)	3172.5 (0.2)	3172.7	3151.6
ν_1	3666.1 (0.4)	3666.0 (0.3)	3656.5 (9.2)	3665.7	3657.1
ν_3	3745.3 (0.8)	3745.3 (0.8)	3723.5 (21.0)	3744.5	3755.9
$3\nu_2$	4701.6 (0.0)	4700.7 (0.9)	4709.9 (8.3)	4701.6	4666.8
$\nu_1\nu_2$	5255.2 (1.0)	5254.9 (0.7)	5225.3 (28.9)	5254.2	5235.0
$\nu_2\nu_3$	5306.9 (1.7)	5306.1 (0.9)	5253.2 (52.0)	5305.2	5331.3
$4\nu_2$	6188.0 (1.6)	6187.9 (1.6)	6210.0 (23.7)	6186.4	6134.0
$\nu_1 2\nu_2$	6807.6 (1.4)	6807.0 (0.9)	6758.5 (47.6)	6806.1	6775.1
$2\nu_2\nu_3$	6833.7 (2.1)	6832.0 (0.4)	6761.6 (70.0)	6831.6	6871.5
$2\nu_1$	7216.6 (1.7)	7216.4 (1.4)	7162.8 (52.1)	7214.9	7201.5
$\nu_1\nu_3$	7250.7 (2.3)	7250.7 (2.3)	7189.9 (58.5)	7248.4	7249.8
$2\nu_3$	7429.2 (1.9)	7429.4 (2.1)	7380.6 (46.7)	7427.3	7445.0
MAD[d]	1.2	1.0	32.4		

The deviations from direct VCI/3MR results are presented in parentheses. Units in cm^{-1}

[a] Multiresoluiton PES based on normal coordinates derived from the CCSD(T) method

[b] Multiresolution PES based on normal coordinates derived from the B3LYP method

[c] Ref. [44]

[d] Mean absolute deviations from direct VCI/3MR results

Hessian matrix, which required 7 and 13 points of Hessian calculations for H_2O and H_2CO, respectively. Note that the QFF based on the B3LYP method can be obtained very efficiently by making use of the analytical Hessian available in many implementations. Spline functions were constructed in the same way as direct PEFs, but with much reduced number of grid points for electronic structure calculations of the energy. In this way, a remarkable speed-up in generating PES was achieved by a factor of 4 and 11 for H_2O and H_2CO, respectively, compared to the direct 3MR-PES. This computational cost reduction is shown to cause only negligibly small errors in the following.

In the present scheme, the normal coordinates of the system need to be computed in advance of the PES scan. The computational cost of this step, which involves the calculations of the equilibrium geometry and the Hessian matrix, grows rapidly with system size, and becomes a severer computational bottleneck than the PES construction. Therefore, it is useful to investigate if the normal coordinates derived from the lower level of theory can be used in defining the PEFs and in the subsequent vibrational state calculations. Indeed, the geometrical parameters and the normal displacement vectors are often obtained with sufficient accuracy by a relatively low level of theory (though the harmonic frequencies are not). This fact has motivated us to construct MultiR-PES in terms of two different normal coordinates derived from the CCSD(T)/cc-pVTZ and B3LYP/cc-pVDZ level of theory (denoted MultiR-PES1 and MultiR-PES2, respectively).

3.2.3 Results

Vibrational energy levels obtained from the VCI method based on MultiR-PES1 and MultiR-PES2 are presented in Tables 2 and 3 for H_2O and H_2CO, respectively, together with direct VCI/2MR and 3MR results, and the experimental values. Table 2 shows that the vibrational energies of H_2O obtained from the two MultiR-PESs are both in excellent agreement with the reference values. The mean absolute errors are 1.2 and 1.0 cm^{-1} for MultiR-PES1 and MultiR-PES2, respectively, and the maximum error is 2.3 cm^{-1}. The accuracy within 3 cm^{-1} is satisfactory at this stage, in view of the fact that the electronic structure method at the CCSD(T)/cc-pVTZ level itself causes an error of $\sim$ 20 cm^{-1} on average. On the other hand, the results of direct VCI/2MR, which neglects the three-mode coupling term, are found with a large mean absolute error of 32.4 cm^{-1}. Therefore, it is essential to include the three-mode coupling term even at least in an approximate manner, i.e., at S7/CCSD/cc-pVDZ level.

The VCI results for H_2CO based on both MultiR-PES1 and MultiR-PES2, as presented in Table 3, are also in excellent agreement with the corresponding direct VCI/3MR results; the mean absolute deviations are 7.6 and 6.9 cm^{-1}, respectively. In contrast, direct VCI/2MR calculation results in large errors. While for some vibrational bands, it gives decent agreement within a few wavenumber, for other bands errors are excessively large. For example, the errors for ν_5

Table 3 Vibrational energy levels of H_2CO obtained from VCI method based on two types of multiresolution PES (MultiR-PES), together with direct VCI/2MR and 3MR results, and the experimental values

	MultiR-PES1[b]	MultiR-PES2[c]	Direct2MR	Direct3MR	Exp.[d]
ν_4	1157.6 (0.1)	1156.9 (0.8)	1155.4 (2.3)	1157.7	1167.4
ν_6	1250.3 (2.7)	1250.8 (3.2)	1247.0 (0.7)	1247.6	1249.6
ν_3	1502.4 (3.5)	1508.7 (2.9)	1504.7 (1.1)	1505.8	1500.2
ν_2	1756.7 (8.0)	1750.5 (1.7)	1749.1 (0.3)	1748.7	1746.1
$2\nu_4$	2308.9 (0.5)	2307.4 (2.0)	2309.1 (0.3)	2309.4	2327.5
$\nu_4\nu_6$	2411.9 (5.2)	2411.3 (4.6)	2402.2 (4.5)	2406.8	2422.4
$2\nu_6$	2497.1 (5.3)	2497.6 (5.8)	2490.4 (1.4)	2491.8	2496.1
$\nu_3\nu_4$	2661.7 (0.3)	2666.8 (4.8)	2657.3 (4.6)	2662.0	2667.1
$\nu_3\nu_6^a$	2694.3 (7.8)	2717.9 (15.8)	2752.5 (50.4)	2702.0	2718.6
ν_1	2775.8 (2.4)	2777.1 (1.1)	2764.7 (13.4)	2778.1	2782.2
ν_5^a	2846.0 (4.9)	2835.7 (5.4)	2773.5 (67.6)	2841.1	2843.0
$\nu_2\nu_4$	2907.7 (9.5)	2899.9 (1.6)	2896.3 (2.0)	2898.3	2906.0
$\nu_2\nu_1$	3004.8 (1.6)	3007.2 (0.9)	2991.0 (15.4)	3006.3	2998.1
$2\nu_3$	3016.9 (6.7)	3016.4 (6.2)	3006.5 (3.7)	3010.2	3000.6
$\nu_2\nu_3$	3253.3 (6.9)	3253.1 (6.7)	3244.3 (2.1)	3246.4	3239.0
$3\nu_4$	3460.0 (0.7)	3457.8 (3.0)	3465.8 (5.1)	3460.7	3471.6
$2\nu_2$	3494.2 (16.6)	3481.0 (3.4)	3479.4 (1.8)	3477.6	3480.7
$2\nu_4\nu_6$	3570.1 (7.5)	3568.4 (5.8)	3557.1 (5.5)	3562.6	3586.6
$\nu_2 2\nu_6$	3665.9 (10.1)	3665.0 (9.1)	3647.8 (8.1)	3655.8	3673.5
$3\nu_6$	3742.3 (7.6)	3742.9 (8.3)	3733.4 (1.3)	3734.7	–
$\nu_3 2\nu_4$	3818.5 (3.1)	3822.4 (7.0)	3810.8 (4.5)	3815.3	3825.3
$\nu_3\nu_4\nu_6^a$	3836.4 (8.7)	3858.1 (12.9)	3871.6 (26.4)	3845.1	3886.5
$\nu_5\nu_6^a$	3912.3 (5.4)	3927.9 (10.2)	3900.4 (17.2)	3917.7	3937.4
$\nu_1\nu_4$	3927.5 (1.8)	3941.3 (12.0)	3908.0 (21.3)	3929.3	3940.2
$\nu_3\nu_4\nu_6^a$	3988.7 (7.3)	3976.4 (4.9)	3975.8 (5.6)	3981.3	3995.8
$\nu_1\nu_6$	4016.2 (1.5)	4019.1 (4.5)	3994.9 (19.8)	4014.7	–
$\nu_2 2\nu_4$	4055.7 (9.9)	4046.2 (0.3)	3997.0 (48.8)	4045.8	4058.3
$\nu_3 2\nu_6$	4086.0 (8.7)	4075.9 (1.4)	4046.0 (31.3)	4077.3	4083.1
$\nu_2\nu_4\nu_6$	4152.0 (5.8)	4161.0 (3.2)	4140.9 (16.8)	4157.7	4163.9
$2\nu_3\nu_4$	4169.0 (2.0)	4178.5 (11.5)	4159.0 (8.1)	4167.0	–
$2\nu_3\nu 6^a$	4172.2 (3.8)	4191.4 (23.0)	4230.7 (62.3)	4168.4	–
$\nu_2 2\nu 6^a$	4242.1 (0.8)	4246.6 (3.7)	4231.4 (11.5)	4242.9	4248.7
$\nu_1\nu_3^a$	4282.9 (6.9)	4273.0 (3.1)	4241.1 (34.9)	4276.0	4253.8
$2\nu_3\nu_6^a$	4347.9 (4.5)	4341.2 (2.2)	4256.1 (87.2)	4343.3	–
$\nu_2\nu_3\nu_4$	4408.6 (11.4)	4406.0 (8.8)	4391.4 (5.8)	4397.2	4397.5
$\nu_2\nu_3\nu_6^a$	4469.3 (3.0)	4476.9 (10.5)	4489.3 (23.0)	4466.3	4466.8
$3\nu_3$	4508.8 (5.5)	4524.4 (10.1)	4507.1 (7.2)	4514.3	–
$\nu_1\nu_2$	4535.9 (5.3)	4530.6 (0.0)	4511.5 (19.0)	4530.6	4529.4
$\nu_2\nu_5^a$	4587.4 (16.9)	4573.6 (3.0)	4518.2 (52.3)	4570.5	4571.5
$2\nu_2\nu_4$	4627.7 (6.5)	4624.0 (2.9)	4620.8 (0.4)	4621.2	4624.3
$4\nu_4$	4640.7 (12.9)	4624.8 (3.0)	4643.3 (15.5)	4627.8	4629.0
$3\nu_4\nu_6$	4741.6 (9.7)	4737.9 (5.9)	4718.9 (13.0)	4732.0	4730.8
$\nu_2 2\nu_3$	4752.3 (7.7)	4747.9 (3.4)	4731.4 (13.1)	4744.5	4733.8
$2\nu_2\nu_6$	4768.0 (17.7)	4756.6 (6.3)	4738.6 (11.7)	4750.3	4741.9
$2\nu_4 2\nu_6$	4844.8 (14.4)	4841.2 (10.8)	4822.3 (8.1)	4830.4	4842.0

Table 3 continued

	MultiR-PES1[b]	MultiR-PES2[c]	Direct2MR	Direct3MR	Exp.[d]
$\nu_4 3\nu_6$	4933.6 (14.5)	4931.1 (11.9)	4911.6 (7.6)	4919.1	–
$2\nu_2\nu_3$	4972.8 (4.1)	4979.7 (11.1)	4966.7 (2.0)	4968.6	4955.2
$\nu_3 3\nu_4$	4987.6 (4.2)	4989.2 (5.8)	4985.7 (2.3)	4983.4	4977.1
$2\nu_4\nu_5^a$	4990.5 (3.7)	4992.3 (5.5)	4985.9 (0.9)	4986.8	–
$4\nu_6$	5002.0 (10.9)	5001.4 (10.3)	4992.8 (1.8)	4991.0	–
$\nu_4\nu_5\nu_6^a$	5064.8 (4.9)	5081.8 (12.0)	5052.0 (17.8)	5069.7	5043.7
$\nu_1 2\nu_4$	5082.6 (1.1)	5088.0 (4.3)	5080.2 (3.5)	5083.7	5092.4
$\nu_3 2\nu_4\nu_6^a$	5146.2 (13.1)	5134.3 (1.2)	5082.9 (50.2)	5133.1	5104.0
$\nu_5 2\nu_6^a$	5149.2 (3.1)	5176.8 (24.5)	5148.4 (3.9)	5152.3	5140.1
$\nu_1\nu_4\nu_6$	5181.7 (5.2)	5182.8 (6.3)	5175.3 (1.2)	5176.5	5151.0
$3\nu_2$	5216.2 (26.8)	5194.6 (5.2)	5186.9 (2.6)	5189.4	5177.6
$\nu_2 3\nu_4$	5219.8 (9.9)	5207.9 (2.0)	5193.8 (16.1)	5209.9	5205.2
$\nu_3\nu_4 2\nu_6^a$	5254.5 (16.0)	5241.7 (3.2)	5218.9 (19.6)	5238.5	5244.1
$\nu_1 2\nu_6$	5261.9 (4.1)	5266.0 (8.2)	5236.7 (21.1)	5257.8	–
$\nu_3\nu_4\nu_5^a$	5303.0 (15.0)	5323.5 (5.5)	5258.2 (59.8)	5318.0	5312.2
$\nu_3 3\nu_6^a$	5312.0 (9.0)	5326.8 (5.8)	5311.9 (9.1)	5321.0	5321.3
$\nu_2 2\nu_4\nu_6^a$	5330.1 (6.8)	5336.2 (12.8)	5331.2 (7.8)	5323.4	5325.6
$\nu_3\nu_5\nu_6^a$	5340.8 (9.3)	5353.7 (22.2)	5333.4 (1.9)	5331.5	5353.2
$2\nu_3 2\nu_4$	5347.5 (9.8)	5361.4 (23.7)	5371.6 (33.9)	5337.7	5389.4
$\nu_1\nu_5^a$	5390.7 (10.8)	5411.1 (9.7)	5386.0 (15.5)	5401.4	–
$\nu_1\nu_3\nu_4^a$	5410.9 (1.5)	5415.4 (5.9)	5386.5 (22.9)	5409.5	5417.6
$\nu_2\nu_4 2_\nu 6^a$	5454.8 (17.3)	5439.5 (2.0)	5403.7 (33.8)	5437.5	5433.4
$2\nu_1^a$	5466.2 (4.5)	5473.2 (2.5)	5434.2 (36.5)	5470.6	5462.7
$2\nu_3\nu_4\nu_6^a$	5513.9 (13.9)	5504.1 (4.1)	5440.0 (60.0)	5500.0	5489.0
$\nu_2 3\nu_6$	5527.0 (16.6)	5515.0 (4.6)	5484.3 (26.1)	5510.4	5530.5
$2\nu_3 2\nu_6^a$	5544.6 (1.1)	5553.6 (7.9)	5490.8 (54.8)	5545.7	5546.5
$\nu_2\nu_3 2\nu_4$	5574.2 (9.9)	5560.4 (3.9)	5521.6 (42.7)	5564.3	5551.3
$\nu_1\nu_3\nu_4^a$	5579.7 (14.1)	5573.3 (7.8)	5552.5 (13.0)	5565.5	–
$\nu_2\nu_4\nu_5^a$	5612.6 (2.6)	5617.3 (7.3)	5562.3 (47.7)	5610.0	5625.5
$2\nu_3\nu_5^a$	5629.5 (23.0)	5650.7 (1.8)	5613.2 (39.3)	5652.5	–
$2\nu_5^a$	5667.9 (4.9)	5677.5 (14.5)	5649.8 (13.2)	5663.0	5651.0
$\nu_1\nu_2\nu_4$	5689.2 (9.0)	5682.1 (1.9)	5661.6 (18.5)	5680.1	5680.0
$3\nu_3\nu_4$	5695.5 (5.7)	5706.6 (16.7)	5682.8 (7.0)	5689.8	–
$\nu_2\nu_5\nu_6^a$	5696.2 (2.6)	5711.0 (17.4)	5692.1 (1.6)	5693.7	5687.9
MAD[e]	7.6	6.9	18.4		

The deviations from direct VCI/3MR results are presented in parentheses. Units in cm^{-1}

[a] The weight of main configuration is less than 0.7

[b] Multiresolution PES based on normal coordinates derived from the CCSD(T) method

[c] Multiresolution PES based on normal coordinates derived from the B3LYP method

[d] Ref. [45]

[e] Mean absolute deviations from the direct VCI/3MR results

and $\nu_3\nu_6$ are found to be 67.6 and 50.4 cm^{-1}. These two states are strongly coupled through the three-mode term,

$$\langle \Psi_{5_1}^{\mathrm{VSCF}} | V | \Psi_{3_1 6_1}^{\mathrm{VSCF}} \rangle = \langle \psi_0^{(3)} \psi_1^{(5)} \psi_0^{(6)} | G_{356} | \psi_1^{(3)} \psi_0^{(5)} \psi_1^{(6)} \rangle, \tag{24}$$

where $\psi_n^{(i)}$ is the nth state of the ith one-mode function in the VSCF approximation. This interaction is well known as Fermi resonance in formaldehyde [11]. The 2MR-PES, however, neglects the three-mode term, G_{356}, and hence cannot account for this resonance, which explains the large error in energies and vibrational wavefunctions. Other bands with large errors also manifest resonance to a varied degree through three-mode interactions. Note that the proposed index is capable of detecting the strong coupling in (3,5,6) as shown in Table 1.

Table 4 The equilibrium geometries of H_2O and H_2CO determined at the B3LYP/cc-pVDZ and CCSD(T)/cc-pVTZ levels of theory, and the zero-point averaged geometry based on the VCI wavefunction obtained from the two MultiR-PESs and direct 3MR-PES

H_2O	B3LYP/cc-pVDZ	CCSD(T)/ cc-pVTZ		Exp.
r_e	0.969	0.959		0.958[a]
θ_e	102.7	103.6		104.4[a]
	VCI/MultiR-PES2	VCI/MultiR-PES1	VCI/direct 3MR	
r_0	0.974	0.974	0.974	0.971[b]
θ_0	103.4	103.4	103.4	104.7[b]
H_2CO	B3LYP/cc-pVDZ	CCSD(T)/ cc-pVTZ		Exp.
r_e(CH)	1.120	1.103		1.111[c]
r_e(CO)	1.204	1.210		1.205[c]
θ_e(HCH)	115.1	116.2		116.1[c]
	VCI/MultiR-PES2	VCI/MultiR-PES1	VCI/direct 3MR	
r_0(CH)	1.117	1.117	1.117	1.117[d]
r_0(CO)	1.213	1.213	1.214	1.207[d]
θ_0(HCH)	116.2	116.2	116.1	116.2[d]

Units in Å and degrees
[a] Ref. [46]
[b] Ref. [47,48]
[c] Ref. [49]
[d] Ref. [50]

It is noteworthy that MultiR-PES2 represented in terms of B3LYP normal coordinates yields the results with miniscule errors for both H_2O and H_2CO. Table 4 presents the zero-point averaged geometries based on the VCI wavefunction obtained from the two MultiR-PESs and direct 3MR-PES for H_2O and H_2CO, together with the equilibrium geometry determined at the B3LYP/cc-pVDZ and CCSD(T)/cc-pVTZ level of theory, and the experimental values. The zero-point averaged geometries obtained from the three PES are all found identical, indicating that the deviation of the equilibrium geometries at the B3LYP/cc-pVDZ and CCSD(T)/cc-pVTZ is circumvented through the PES scan. The resulting zero-point averaged geometry is in good agreement with the experimental values for both H_2O and H_2CO. This fact implies that a significant computational saving can be achieved using the normal coordinates of a lower level of theory bypassing the geometry optimization and the Hessian calculation at the higher level of theory.

4 Conclusions

With the intrinsic mode coupling terms presented and implemented in this work, the *n*MR-PES is generated from a set of piecewise reduced dimensional PEFs, each of which can be evaluated by separate and approximate functional form and/or electronic structure method, enabling an optimum control of accuracy–cost trade-off. Three types of functional forms have been explored in representing the piecewise PEFs, i.e., direct PEF (a grid representation), spline interpolation function, and Taylor expansion PEF. QFF, which is a Taylor expansion PEF truncated at the fourth order, is used in the context of multiresolution PES, and has been shown to be highly cost-effective. The newly proposed index provides rapid estimates of the strengths of the mode coupling terms in advance of full calculations of the PES. These indices will be crucial in larger systems, of which the number of mode-coupling terms is large.

The applications to H_2O and H_2CO have attested to the proposed method's effectiveness. Multiresolution PES for these molecules has been constructed by combining the mode coupling terms represented in various resolutions. With the aid of the newly proposed index, the mode coupling terms, classified into five categories, have been assigned their resolution according to the importance. The less important terms have been approximated by progressively coarser-grid spline functions determined at lower level of electronic structure theory. The "very weak" terms were expressed by the QFF. These multiresolution PEFs have enabled a remarkable reduction in computational cost without notable loss of accuracy. The most efficient scheme has reproduced the vibrational frequencies of formaldehyde obtained from 3MR-PES with less than 10% of the cost of the conventional calculation with a mean absolute error less than $10\,cm^{-1}$. The use of normal coordinates determined by a lower level of theory (i.e., B3LYP/cc-pVDZ) has also been explored in defining the PES and in the vibrational state calculations. This scheme is found useful which enables a computational reduction bypassing the geometry optimization and Hessian calculations at a higher level of theory without losing the accuracy.

Acknowledgments One of the authors (SH) thanks financial support from the US Department of Energy (Grant No. DE-FG02-04ER15621) and from the University of Florida Division of Sponsored Research. We thank Dr. A. Perera and Prof. R. J. Bartlett for kindly providing us with the ACES II program.

Appendix A: On Eq. (3)

Assume that Eq. (3) holds for each of the mode coupling term up to the $(m-1)$-th order. Then, the m-mode coupling term with $Q_{i_m}=0$ reads,

$$V_{\mathbf{i}_m}(Q_{i_1},\ldots,Q_{i_{m-1}},0)=V(0,\ldots,Q_{i_1},\ldots,Q_{i_m}=0,\ldots,0)-\sum_{l=1}^{m-1}\sum_{\mathbf{i}_l\in\mathbf{i}_{m-1}}V_{\mathbf{i}_l}(Q_{i_1},\ldots,Q_{i_l}). \tag{A.1}$$

Note that the compound index $\mathbf{i}_l$ that includes i_m can be removed from the summation in the second term because $V_{\mathbf{i}_l}$ is zero. From Eq. (3), $V_{\mathbf{i}_{m-1}}$ is written as,

$$V_{\mathbf{i}_{m-1}}(Q_{i_1},\ldots,Q_{i_{m-1}})=V(0,\ldots,Q_{i_1},\ldots,Q_{i_{m-1}},\ldots,0)-\sum_{l=1}^{m-2}\sum_{\mathbf{i}_l\in\mathbf{i}_{m-1}}V_{\mathbf{i}_l}(Q_{i_1},\ldots,Q_{i_l}). \tag{A.2}$$

Substituting,

$$\sum_{l=1}^{m-1}\sum_{\mathbf{i}_l\in\mathbf{i}_{m-1}}V_{\mathbf{i}_l}=\sum_{l=1}^{m-2}\sum_{\mathbf{i}_l\in\mathbf{i}_{m-1}}V_{\mathbf{i}_l}+V_{\mathbf{i}_{m-1}} \tag{A.3}$$

into Eq. (A.1) and using Eq. (A.2), we find,

$$V_{\mathbf{i}_m}(Q_{i_1},\ldots,Q_{i_{m-1}},0)=V_{\mathbf{i}_{m-1}}-V_{\mathbf{i}_{m-1}}=0. \tag{A.4}$$

It can be proven that $V_{\mathbf{i}_m}$ is zero if any $Q_{i_k}=0$ by simply exchanging the indices i_k and i_m. Thus, if Eq. (3) holds for each mode coupling term up to the $(m-1)$-th order, it also holds for the m-th order coupling terms.

Since Eq. (3) is evident for the one-mode term ($m=1$), it is deduced that Eq. (3) holds for every m.

References

1. Herman M, Lievin J, Auwera JV, Campargue A (1999) Global and accurate vibration hamiltonians from high-resolution molecular spectroscopy. Wiley, New York
2. Bowman JM (1978) J Chem Phys 68:608
3. Gerber RB, Ratner MA (1979) Chem Phys Lett 68:195
4. Bowman JM (1986) Acc Chem Res 19:202
5. Bowman JM, Carter S, Huang X (2003) Int Rev Phys Chem 22:533
6. Gerber RB, Ratner MA (1998) Adv Chem Phys 70:97
7. Christiansen O (2004) J Chem Phys 120:2149
8. Carter S, Culik SJ, Bowman JM (1997) J Chem Phys 107:10458
9. Chaban GM, Jung JO, Gerber RB (1999) J Chem Phys 111:1823
10. Matsunaga N, Chaban GM, Gerber RB (2002) J Chem Phys 117:3541
11. Yagi K, Taketsugu T, Hirao K, Gordon MS (2000) J Chem Phys 113:1005
12. Irle S, Bowman JM (2000) J Chem Phys 113:8401
13. Burcl R, Carter S, Handy NC (2003) Chem Phys Lett 373:357
14. Barone V (2004) J Chem Phys 120:3059
15. Barone V (2005) J Chem Phys 122:014108
16. Yagi K, Hirao K, Taketsugu T, Schmidt MW, Gordon MS (2004) J Chem Phys 121:1383
17. Taketsugu T, Yagi K, Gordon MS (2005) Int J Quant Chem 104:758
18. Bürger H, Kuna R, Ma S, Breidung J, Thiel W (1994) J Chem Phys 101:1
19. Bürger H, Ma S, Breidung J, Thiel W (1996) J Chem Phys 104:4945
20. Boese AD, Martin JML (2004) J Phys Chem A 108:3085
21. Begue D, Carbonniere P, Pouchan C (2005) J Phys Chem A 109:4611
22. Kongsted J, Christiansen O (2006) J Chem Phys 125:124108
23. Xie T, Bowman JM (2002) J Chem Phys 117:10487
24. Carter S, Handy NC (2002) Chem Phys Lett 352:1
25. Carter S, Bowman JM, Braams BJ (2001) Chem Phys Lett 342:636
26. Rauhut G (2004) J Chem Phys 121:9313
27. Pfluger K, Paulus M, Jagiella S, Burkert T, Rauhut G (2005) Theor Chem Acc 114:327
28. Hrenar T, Werner HJ, Rauhut G (2005) Phys Chem Chem Phys 7:3123
29. Yagi K, Taketsugu T, Hirao K (2002) J Chem Phys 116:3963
30. Yagi K, Oyanagi C, Taketsugu T, Hirao K (2003) J Chem Phys 118:1653
31. Oyanagi C, Yagi K, Hirao K, Taketsugu T (2006) J Chem Phys 124:064311
32. Maeda S, Watanabe Y, Ohno K (2005) Chem Phys Lett 414:265
33. Rheinecker JL, Bowman JM (2006) J Chem Phys 124:131102
34. Rheinecker J, Bowman JM (2006) J Chem Phys 125:133206
35. Light JC, Carrington T (2000) Adv Chem Phys 114:263
36. Becke AD (1993) J Chem Phys 98:5648
37. Lee C, Yang W, Parr RG (1988) Phys Rev B 37:785
38. Bartlett RJ (1995) In: Yarkony DR (ed) Modern electronic structure theory, vol II. World Scientific, Singapore
39. Hirata S, Bartlett RJ (2000) Chem Phys Lett 321:216
40. Dunning TH Jr (1989) J Chem Phys 90:1007
41. Stanton JF, Gauss J, Watts JD, Nooijen M, Oliphant N, Perera SA, Szalay PG, Lauderdale WJ, Kucharske SA, Gwaltney SR, Beck S, Balková A, Bernholdt DE, Baeck KK, Rozyczko P, Sekino H, Hober C, Bartlett RJ, ACES2, Quantum Theory Project, University of Florida
42. Frisch MJ et al (2004) Gaussian 03, Revision C.02, Gaussian, Wallingford
43. Yagi K (2006) SINDO, University of Tokyo, Tokyo
44. Tennyson J, Zobov NF, Williamson R, Polyansky OL, Bernath PF (2001) J Phys Chem Ref Data 30:735
45. Bouwens RJ, Hammerschmidt JA, Grzeskowiak MM, Stegink TA, Yorba PM, Polik WF (1996) J Chem Phys 104:460
46. Benedict WS, Gailar N, Plyler EK (1956) J Chem Phys 24:1139
47. Mas EM, Szalewicz K (1996) J Chem Phys 104:7606
48. Kuchitsu K, Kern CW (1962) J Chem Phys 36:2460
49. Gurvich LV, Veyts IV, Alcock CB (1989) Thermodynamic properties of individual substances, 4th edn. Hemisphere Publishing, New York
50. Duncan JL (1974) Mol Phys 28:1177